Bioconjugate Chemistry

Article

pubs.acs.org/bc

# Mapping Peptide Thiol Accessibility in Membranes Using a Quaternary Ammonium Isotope-Coded Mass Tag (ICMT)

Chiao-Yung Su,[†] Erwin London,[†,§] and Nicole S. Sampson*[,†]

[†]Department of Chemistry, Stony Brook University, Stony Brook, New York 11794-3400, United States

[§]Department of Biochemistry and Cell Biology, Stony Brook University, Stony Brook, New York 11794-5215, United States

Supporting Information

**ABSTRACT:** The plasma membrane contains a diverse array of proteins, including receptors, channels, and signaling complexes, that serve as decision-making centers. Investigation of membrane protein topology is important for understanding the function of these types of protein. Here, we report a method to determine protein topology in the membrane that utilizes labeling of cysteine with isotope-coded mass tags. The mass tags contain a thiol reactive moiety, linker, and a quaternary ammonium group to aid ionization in the mass spectrometer and were synthesized in both light and heavy (deuterated) forms. The probes were found to be membrane impermeable when applied to lipid vesicles. To assess the utility of the probes for mapping peptide thiol topology, we employed a two-step labeling procedure. Vesicles containing $\alpha$-helical transmembrane peptides were labeled with heavy (or light) probe, solubilized by detergent, and then labeled by an excess of the complementary probe. Peptide for which the cysteine was oriented in the center of the lipid bilayer was not labeled until the lipid vesicles were lysed with detergent, consistent with the membrane impermeability of the probes and reduced ionization of the thiol in the hydrophobic membrane. Peptide for which the cysteine was positioned in the headgroup zone of the lipid bilayer was labeled rapidly. Peptide for which the cysteine was positioned below the headgroup abutting the hydrocarbon region was labeled at a reduced rate compared to the fully accessible cysteine. Moreover, the effect of lipid bilayer structure on the kinetics of peptide and lipid flipping in the bilayer was readily measured with our two-step labeling method. The small sample size required, the ease and rapidity of sample preparation, and the amenability of MALDI-TOF mass spectral analysis to the presence of lipids will enable future facile investigation of membrane proteins in a cellular context.

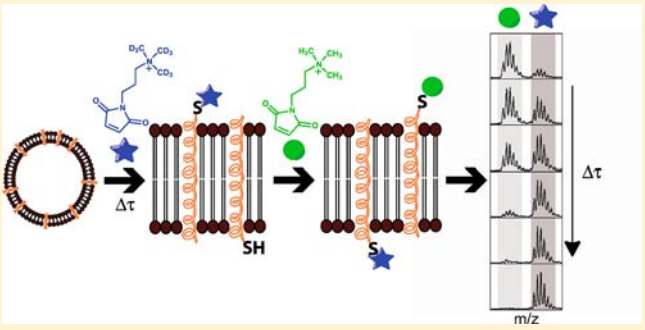


## INTRODUCTION

The biological membrane plays a pivotal role in living systems. The plasma membrane contains a diverse array of proteins, including receptors, channels, and signaling complexes, that serve as an initial decision-making center for the cell.[1] The structures, and thus the functions, of membrane-associated proteins are influenced by their environment in the membrane. However, elucidation of protein structure in the presence of lipids, let alone dynamics in topology, is still a considerable challenge for structural biology.

X-ray structural analysis is limited to those cases for which crystals can be obtained in the presence of detergents and/or lipids. Moreover, the need for crystals impedes study of the influence of different lipids on structure. Methods based on EPR,[2−4] NMR,[5,6] or fluorescence spectroscopy[7] have wider utility. However, both EPR and fluorescence spectroscopies require attachment of probes to the protein of interest. These methods report on environment local to a probe that is often separated from the modified amino acid by a linker. Although orthogonal ligation strategies are available, typically, the spectroscopic probe is introduced at a single site. Therefore, monitoring structural changes in a large protein requires preparation of multiple labeled proteins, each modified at a single unique site, and the probe-linker structure can interfere with interpretation of results.

Substituted-cysteine accessibility methods (SCAM),[8,9] which circumvent the limitations of probe structures, are widely utilized. For example, conjugation of cysteines with membrane-impermeable PEGylation[10−12] reagents in combination with SDS-PAGE allows determination of which cysteines are buried in the membrane and which are accessible. This method yields topology data on either native cysteines or those introduced by mutagenesis.

In contrast, NMR spectroscopy provides simultaneous structural information on an entire protein. The major limit of NMR methods is the quantities of protein required and whether suitable lipid model membrane systems can be found to enable structure determination.

Because of the limitations in currently available protein−lipid topology methods, we sought a mass spectral method that

**Received:** April 5, 2013
**Revised:** May 9, 2013
**Published:** June 2, 2013

could be employed in combination with a SCAM covalent modification strategy. Mass spectrometry has recently become a popular method of analyzing protein topology because of its sensitivity, the introduction of methods to provide relative quantities of species, and the widespread availability of instrumentation to undertake the analysis. We focused on MALDI because the ionization method is less susceptible to lipid and detergent interference than electrospray methods.

In our work, we reasoned that cysteine accessibility could be monitored by comparing labeling of the native protein state in a membrane environment to labeling of the denatured state. Incorporation of heavy isotope into one of the labeling steps would provide accurate and precise measurements of protein topology in a lipid environment. Here we report the design and synthesis of maleimide labeling reagents that include heavy isotope tags and quaternary ammonium moieties for facile gas phase ionization by MALDI-TOF mass spectrometry (Figure 1). We experimentally validated the use of these probes in

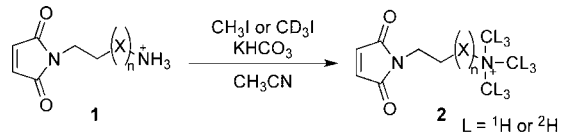


**1a**: X = $CH_2$, n = 1
**1b**: X = $CH_2$, n = 2
**1c**: X = $CH_2$, n = 4
**1d**: X = $OCH_2CH_2$, n = 2

**2a-$d_0$, 2a-$d_9$**: X = $CH_2$, n = 1
**2b-$d_0$, 2b-$d_9$**: X = $CH_2$, n = 2
**2c-$d_0$, 2c-$d_9$**: X = $CH_2$, n = 4
**2d-$d_0$, 2d-$d_9$**: X = $OCH_2CH_2$, n = 2

**Figure 1.** Preparation of ICMT probes. Maleimide **1** was prepared in 3 steps from mono-BOC-protected diamine and maleic anhydride. Permethylation[17] of the maleimide amine **1** with iodomethane-$d_0$ ($CH_3I$) or iodomethane-$d_3$ ($CD_3I$) under mild basic conditions provides probes **2a-$d_0$**–**2d-$d_0$** or **2a-$d_9$**–**2d-$d_9$**, respectively, in 51–90% yield.

membrane topology experiments with both thiolipids and thiol-containing peptides. We demonstrate that the ICMT probes are readily prepared in gram quantities, are not membrane permeable, and react efficiently and rapidly with solvent-accessible thiols. Moreover, their application in kinetics labeling experiments illustrates their utility for monitoring protein topology changes on the second time scale. Ultimately, we envision that this method will be amenable for use in a cellular membrane context.

## EXPERIMENTAL PROCEDURES

**Materials and Reagents.** Solvents were purified with a Pure Process Technology push still system. α-Cyano-4-hydroxycinnamic acid, Triton X-100, and 5(6)-carboxyfluorescein were purchased from Sigma-Aldrich (St. Louis, MO). DL-Dithiothreitol and sodium dodecyl sulfate were purchased from Fisher Scientific (Pittsburgh, PA). Cholic acid sodium salt was obtained from MP Biochemicals, Inc. (Solon, Ohio). Phospholipids were purchased from Avanti Polar Lipids, Inc. (Alabaster, AL). Peptide **3** (Ac-$K_2GL_7WLCL_9K_2A$-$NH_2$), peptide **4** (Ac-$CK_2GL_7WLAL_9K_2A$-$NH_2$), and peptide **5** (Ac-$K_2CL_7WLAL_9K_2A$-$NH_2$) were synthesized by the Keck Laboratory at Yale University. NB-ECD-OMe (5-norbornene-*exo*-carboxyl-glutamate-cysteine-aspartate-α-methyl ester) was synthesized by solution phase methods.[13] Iodomethane-$d_3$ was purchased from Cambridge Isotope Laboratories, Inc. (Andover, MA).

The synthesis of *tert*-butyl-aminoalkyl carbamates, **11**, was performed according to the procedure of Guy et al.[14] The syntheses of compounds **12** and **13** were performed following a modification of the procedure to prepare *N*-ethyl maleimide reported by Niwayama et al.[15] as outlined below (Figure 2).

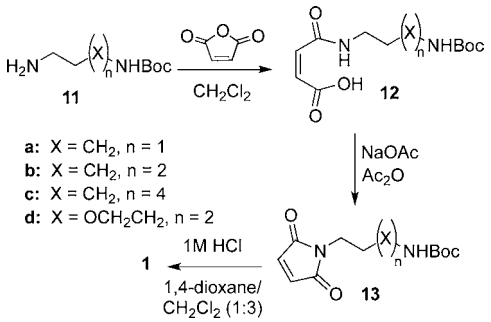


**Figure 2.** Synthetic route for the preparation of ICMT maleimide precursors **1a**–**1d**.

Analytical thin layer chromatography (TLC) was performed on precoated silica gel plates (60F254), flash chromatography on silica gel-60 (230–400 mesh), and Combi-Flash chromatography on RediSep normal phase silica columns (silica gel-60, 230–400 mesh). Inova 400, Inova 500, Inova 600, and Bruker 400 MHz NMR spectrometers and a PTI spectrofluorimeter were used for analysis. $^1$H NMR spectra are reported as chemical shift in parts per million (ppm) (multiplicity, coupling constant in Hz, and integration). $^{13}$C NMR spectra are reported as chemical shifts in ppm. The solvent peak was used as an internal reference.

*4-(3-(tert-Butoxycarbonylamino)propylamino)-4-oxobut-2-enoic acid (**12a**):*[15] *tert*-Butyl 3-aminopropylcarbamate (**11a**)[14] (11.65 g, 66.9 mmol) in $CH_2Cl_2$ (100 mL) was added dropwise to ice cooled maleic anhydride (6.56 g, 66.9 mmol) in $CH_2Cl_2$ (150 mL). The solution was stirred for 3 h and was washed with saturated NaCl solution and $H_2O$. The organic layer was dried over $Na_2SO_4$, and solvent was removed under reduced pressure. The product was further purified by column chromatography (linear gradient elution: hexane/EtOAc, 85/15 to 20/80). Yield: 94%. $^1$H NMR (500 MHz, $CDCl_3$) δ 8.23 (s, 1H), 6.36 (d, *J* = 10.0 Hz, 1H), 6.32 (d, *J* = 10.0 Hz, 1H), 4.84 (s, 1H), 3.40 (td, *J* = 10.0 and 5.0 Hz, 2H), 3.22 (td, *J* = 10.0 and 5.0 Hz, 2H), 1.70 (q, *J* = 5.0 Hz, 2H), 1.45 (s, 9H); $^{13}$C NMR (100 MHz, $CD_3OD$) δ 168.12, 168.03, 158.72, 134.40, 133.50, 80.21, 38.83, 38.46, 30.29, 28.89. MS (ESI) Calcd. for $C_{12}H_{20}N_2O_5$ $(MNa)^+$: 295.13; Found: 295.23.

*4-(4-(tert-Butoxycarbonylamino)butylamino)-4-oxobut-2-enoic acid (**12b**).* Compound **12b** was prepared by the same method as **12a** starting from *tert*-butyl (4-aminobutyl)-carbamate (**11b**) and maleic anhydride. Yield: 89%. $^1$H NMR (400 MHz, $CDCl_3$) δ 8.68 (s, 1H), 6.49 (d, *J* = 12.0 Hz, 1H), 6.30 (d, *J* = 12.0 Hz, 1H), 4.82 (s, 1H), 3.39 (td, *J* = 8.0 and 4.0 Hz, 2H), 3.15 (td, *J* = 8.0 and 5.0 Hz, 2H), 1.70–1.50 (m, 4H), 1.43 (s, 9H); $^{13}$C NMR (100 MHz, $CDCl_3$) δ 166.25, 165.95, 156.79, 135.62, 131.97, 79.77, 40.29, 39.58, 28.37, 24.59. MS (ESI) Calcd. for $C_{13}H_{22}N_2O_5$ $(MNa)^+$: 309.14; Found: 309.24.

*4-(6-(tert-Butoxycarbonylamino)hexylamino)-4-oxobut-2-enoic acid (**12c**).* Compound **12c** was prepared by the same method as **12a** starting from *tert*-butyl (6-aminohexyl)-carbamate (**11c**) and maleic anhydride. Yield: 69%. $^1$H NMR (400 MHz, $CDCl_3$) δ 8.39 (s, 1H), 6.51 (d, *J* = 12.0 Hz, 1H),


dx.doi.org/10.1021/bc400171j | Bioconjugate Chem. 2013, 24, 1235–1247

6.28 (d, $J$ = 12.0 Hz, 1H), 4.73 (t, $J$ = 8.0 Hz, 1H), 3.39 (td, $J$ = 8.0 and 4.0 Hz, 2H), 3.10 (d, $J$ = 8.0 Hz, 2H), 1.59 (td, $J$ = 8.0 and 4.0 Hz, 2H), 1.50−1.25 (m, 6H), 1.42 (s, 9H); $^{13}$C NMR (100 MHz, $CDCl_3$) $\delta$ 166.21, 166.03, 056.53, 135.49, 132.12, 79.34, 39.66, 29.87, 28.38, 28.09, 25.44, 25.20. MS (ESI) Calcd. for $C_{15}H_{26}N_2O_5$ $(MNa)^+$: 337.17; Found: 337.31.

*2,2-Dimethyl-4,15-dioxo-3,8,11-trioxa-5,14-diazaoctadec-16-en-18-oic acid (**12d**).* Compound **12d** was prepared by the same method as **12a** starting from *tert*-butyl (2-(2-(2-aminoethoxy)ethoxy)ethyl)carbamate (**11d**) and maleic anhydride. Yield: 95%. $^1$H NMR (400 MHz, $CDCl_3$) $\delta$ 6.49 (d, $J$ = 12.8 Hz, 1H), 6.26 (d, $J$ = 12.4 Hz, 1H), 3.65−3.60 (m, 6H), 3.50 (q, $J$ = 6.0 Hz, 4H), 3.22 (t, $J$ = 5.6 Hz, 2H), 1.43 (s, 9H); $^{13}$C NMR (100 MHz, $CD_3OD$) $\delta$ 168.02, 167.96, 158.53, 134.07, 133.89, 80.22, 71.44, 71.19, 70.03, 54.95, 41.31, 41.06, 28.89. MS (ESI) Calcd. for $C_{15}H_{26}N_2O_7$ $(MNa)^+$: 369.16; Found: 369.23.

*tert-Butyl 3-(2,5-dioxo-2H-pyrrol-1(5H)-yl)-propylcarbamate (**13a**).*[15] A mixture of **12a** (4.52 g, 16.60 mmol), anhydrous sodium acetate (1.23 g, 14.94 mmol), and acetic anhydride (22.03 g, 215.80 mmol) was heated at 110 °C for 3 h. After the reaction was complete, it was cooled to 22 °C, and an ice cold saturated $NaHCO_3$ solution was poured into the reaction mixture to neutralize excess acetic anhydride and acetic acid. The mixture was extracted with $CH_2Cl_2$, washed with brine and $H_2O$, and dried over $Na_2SO_4$. After evaporation of the solvent, the product was purified by column chromatography (linear gradient elution: hexane/EtOAc, 95/5 to 60/40). Yield: 60%. $^1$H NMR (400 MHz, $CDCl_3$) $\delta$ 6.69 (s, 2H), 4.90 (s, 1H), 3.57 (t, $J$ = 6.8 Hz, 2H), 3.07 (q, $J$ = 6.4 Hz, 2H), 1.74 (q, $J$ = 6.4 Hz, 2H), 1.43 (s, 9H); $^{13}$C NMR (100 MHz, $CDCl_3$) $\delta$ 170.87, 155.83, 134.11, 79.21, 37.31, 34.95, 28.79, 28.35. MS (ESI) Calcd. for $C_{12}H_{18}N_2O_4$ $(MNa)^+$: 277.12; Found: 277.21.

*tert-Butyl 4-(2,5-dioxo-2H-pyrrol-1(5H)-yl)butylcarbamate (**13b**).* Compound **13b** was prepared by the same method as **13a** starting from **12b**. Yield: 55%. $^1$H NMR (400 MHz, $CDCl_3$) $\delta$ 6.68 (s, 2H), 4.54 (s, 1H), 3.52 (t, $J$ = 8.0 Hz, 2H), 3.12 (d, $J$ = 4.0 Hz, 2H), 1.61 (q, $J$ = 8.0 Hz, 2H), 1.46 (m, 2H), 1.42 (s, 9H); $^{13}$C NMR (100 MHz, $CDCl_3$) $\delta$ 170.67, 155.81, 133.98, 78.99, 39.88, 37.34, 28.30, 27.26, 25.78. MS (ESI) Calcd. for $C_{13}H_{20}N_2O_4$ $(MNa)^+$: 291.13; Found: 291.24.

*tert-Butyl 6-(2,5-dioxo-2H-pyrrol-1(5H)-yl)hexylcarbamate (**13c**).* Compound **13c** was prepared by the same method as **13a** starting from **12c**. Yield: 65%. $^1$H NMR (600 MHz, $CDCl_3$) $\delta$ 6.65 (s, 2H), 4.53 (s, 1H), 3.47 (t, $J$ = 7.2 Hz, 2H), 3.06 (d, $J$ = 6.0 Hz, 2H), 1.54 (q, $J$ = 7.2 Hz, 2H), 1.43 (m, 2H), 1.40 (s, 9H), 1.23−1.33 (m, 4H); $^{13}$C NMR (100 MHz, $CDCl_3$) $\delta$ 170.77, 155.91, 133.97, 78.94, 40.36, 37.65, 29.83, 28.35, 26.28, 26.15. MS (ESI) Calcd. for $C_{15}H_{24}N_2O_4$ $(MNa)^+$: 319.16; Found: 319.28.

*tert-Butyl 2-(2-(2-(2,5-dioxo-2H-pyrrol-1(5H)-yl)ethoxy)-ethoxy)ethylcarbamate (**13d**).* Compound **13d** was prepared by the same method as **13a** starting from 2,2-dimethyl-4,15-dioxo-3,8,11-trioxa-5,14-diazaoctadec-16-en-18-oic acid (**12d**). Yield: 65%. $^1$H NMR (500 MHz, $CDCl_3$) $\delta$ 6.70 (s, 2H), 5.00 (s, 1H), 3.73 (t, $J$ = 5.5 Hz, 2H), 3.64 (t, $J$ = 6.0 Hz, 2H), 3.59 (q, $J$ = 3.0 Hz, 2H), 3.54 (q, $J$ = 3.0 Hz, 2H), 3.49 (t, $J$ = 5.0 Hz, 2H), 3.28 (d, $J$ = 4.5 Hz, 2H), 1.43 (s, 9H); $^{13}$C NMR (100 MHz, $CDCl_3$) $\delta$ 170.53, 155.84, 134.05, 79.04, 70.12, 69.79, 67.69, 40.32, 36.93, 28.31. MS (ESI) Calcd. for $C_{15}H_{24}N_2O_6$ $(MNa)^+$: 351.15; Found: 351.21.

*3-(2,5-Dioxo-2H-pyrrol-1(5H)-yl)propan-1-aminium chloride (**1a**).*[16] Compound **13a** (3.54 g, 13.92 mmol) was dissolved in $CH_2Cl_2$ (40 mL) at 22 °C. 4 M HCl in 1,4-dioxane (15 mL) was added and the solution was stirred at 22 °C for 2 h. The solvent was removed under reduced pressure, and the residue was dried under high vacuum. Yield: 100%. $^1$H NMR (500 MHz, $D_2O$) $\delta$ 6.92 (s, 2H), 3.67 (t, $J$ = 7.0 Hz, 2H), 3.06 (t, $J$ = 7.0 Hz, 2H), 2.00 (q, $J$ = 7.0 Hz, 2H). MS (ESI) Calcd. for $C_7H_{11}N_2O_2^+$ $(MH)^+$: 155.08; Found: 155.10.

*4-(2,5-Dioxo-2H-pyrrol-1(5H)-yl)butan-1-aminium chloride (**1b**).* Compound **1b** was prepared by the same method as **1a** starting from **13b**. Yield: 100%. $^1$H NMR (500 MHz, $D_2O$) $\delta$ 6.90 (s, 2H), 3.60 (t, $J$ = 7.0 Hz, 2H), 3.05−3.10 (m, 2H), 1.70 (m, 4H). MS (ESI) Calcd. for $C_8H_{13}N_2O_2^+$ $(MH)^+$: 169.10; Found: 169.09.

*6-(2,5-Dioxo-2H-pyrrol-1(5H)-yl)hexan-1-aminium chloride (**1c**).* Compound **1c** was prepared by the same method as **1a** starting from **13c**. Yield: 100%. $^1$H NMR (400 MHz, $D_2O$) $\delta$ 6.60 (s, 2H), 3.25 (t, $J$ = 5.6 Hz, 2H), 2.75 (t, $J$ = 7.6 Hz, 2H), 1.41 (p, $J$ = 7.6 Hz, 2H), 1.32 (p, $J$ = 7.6 Hz, 2H), 1.15 (p, $J$ = 7.6 Hz, 2H), 1.05 (p, $J$ = 6.8 Hz, 2H). MS (ESI) Calcd. for $C_{10}H_{17}N_2O_2^+$ $(MH)^+$: 197.13; Found: 197.10.

*2-(2-(2-(2,5-Dioxo-2H-pyrrol-1(5H)-yl)ethoxy)ethoxy)-ethanaminium chloride (**1d**).* Compound **1d** was prepared by the same method as **1a** starting from **13d**. Yield: 100%. $^1$H NMR (500 MHz, $D_2O$) $\delta$ 6.91 (s, 2H), 3.70−3.80 (m, 10H), 3.23 (t, $J$ = 5.0 Hz, 2H). MS (ESI) Calcd. for $C_{10}H_{17}N_2O_4^+$ $(MH)^+$: 229.12; Found: 229.11.

*3-(2,5-Dioxo-2H-pyrrol-1(5H)-yl)-N,N,N-trimethylpropan-1-aminium iodide (**2a-d$_0$**).*[17] A mixture of **1a** (2.65 g, 13.9 mmol), iodomethane (9.9 g, 70 mmol), and $KHCO_3$ (7.0 g, 70 mmol) in ACN was stirred at 22 °C under $N_2$ for 72 h. Solids were removed by filtration, and the solvent was removed from the filtrate under reduced pressure. Maleimide **2a-d$_0$** was recrystallized from ethanol. Yield: 71%. $^1$H NMR (500 MHz, $D_2O$) $\delta$ 6.92 (s, 2H), 3.68 (t, $J$ = 6.5 Hz, 2H), 3.41 (td, $J$ = 4.5 and 4.0 Hz, 2H), 3.15 (s, 9H), 2.16 (tt, $J$ = 8.0 and 6.5 Hz, 2H); $^{13}$C NMR (100 MHz, $D_2O$) $\delta$ 172.91, 134.61, 64.01, 53.12, 34.48, 22.13. mp = 183−183.5 °C. MS (ESI) Calcd. for $C_{10}H_{17}N_2O_2^+$ $(M^+)$: 197.13; Found: 197.16.

*3-(2,5-Dioxo-2H-pyrrol-1(5H)-yl)-N,N,N-trimethyl-d$_9$-propan-1-aminium iodide (**2a-d$_9$**).*[17] A mixture of **1a** (2.74 g, 14.4 mmol), iodomethane-$d_3$ (12.48 g, 86.1 mmol), and $KHCO_3$ (8.62 g, 86.1 mmol) in ACN was stirred at 22 °C under $N_2$ for 72 h. Solids were removed by filtration, and the solvent was removed from the filtrate under reduced pressure. Maleimide **2a-d$_9$** was recrystallized from EtOH. Yield: 78%. $^1$H NMR (400 MHz, $D_2O$) $\delta$ 6.95 (s, 2H), 3.71 (t, $J$ = 6.6 Hz, 2H), 3.45 (td, $J$ = 4.7 and 3.6 Hz, 2H), 2.19 (tt, $J$ = 8.8 and 6.6 Hz, 2H); $^{13}$C NMR (100 MHz, $D_2O$) $\delta$ 172.93, 134.65, 63.74, 52.27, 34.53, 22.12. mp = 182−183 °C. MS (ESI) Calcd. for $C_{10}H_8D_9N_2O_2^+$ $(M^+)$: 206.18; Found: 205.99.

*4-(2,5-Dioxo-2H-pyrrol-1(5H)-yl)-N,N,N-trimethylbutan-1-aminium iodide (**2b-d$_0$**).* Compound **2b-d$_0$** was prepared by the same method as **2a-d$_0$** starting from **1b** and iodomethane. Yield: 74%. $^1$H NMR (400 MHz, $D_2O$) $\delta$ 6.92 (s, 2H), 3.63 (t, $J$ = 6.7 Hz, 2H), 3.42 (td, $J$ = 5.0 and 4.5 Hz, 2H), 3.17 (s, 9H), 1.84 (tt, $J$ = 8.5 and 7.1 Hz, 2H), 1.71 (q, $J$ = 7.0 Hz, 2H); $^{13}$C NMR (100 MHz, $D_2O$) $\delta$ 173.27, 134.48, 65.91, 53.03, 36.71, 24.65, 19.81. mp = 182−182.5 °C. MS (ESI) Calcd. for $C_{11}H_{19}N_2O_2^+$ $(M^+)$: 211.14; Found: 211.17.

*4-(2,5-Dioxo-2H-pyrrol-1(5H)-yl)-N,N,N-trimethyl-d$_9$-butan-1-aminium iodide (**2b-d$_9$**).* Compound **2b-d$_9$** was


dx.doi.org/10.1021/bc400171j | Bioconjugate Chem. 2013, 24, 1235−1247

prepared by the same method as **2a-d$_9$** starting from **1b** and iodomethane-$d_3$. Yield: 82%. $^1$H NMR (400 MHz, $D_2O$) $\delta$ 6.90 (s, 2H), 3.62 (t, $J$ = 6.7 Hz, 2H), 3.40 (td, $J$ = 4.5 and 4.0 Hz, 2H), 1.82 (tt, $J$ = 8.5 and 7.1 Hz, 2H), 1.70 (q, $J$ = 7.0 Hz, 2H); $^{13}$C NMR (100 MHz, $D_2O$) $\delta$ 173.26, 134.45, 65.60, 51.96, 36.66, 24.62, 19.71. mp = 175−176 °C. MS (ESI) Calcd. for $C_{11}H_{10}D_9N_2O_2^+$ ($M^+$): 220.20; Found: 220.03.

*6-(2,5-Dioxo-2H-pyrrol-1(5H)-yl)-N,N,N-trimethylhexan-1-aminium iodide (**2c-d$_0$**).* Compound **2c-d$_0$** was prepared by the same method as **2a-d$_0$** starting from **1c** and iodomethane. Yield: 70%. $^1$H NMR (600 MHz, $D_2O$) $\delta$ 6.90 (s, 2H), 3.56 (t, $J$ = 6.6 Hz, 2H), 3.36 (td, $J$ = 5.4 and 4.2 Hz, 2H), 3.16 (s, 9H), 1.83 (q, $J$ = 7.2 Hz, 2H), 1.65 (q, $J$ = 7.2 Hz, 2H), 1.38−1.46 (m, 4H); $^{13}$C NMR (125 MHz, $D_2O$) $\delta$ 176.11, 136.98, 69.24, 55.47, 40.06, 29.99, 28.03, 27.57, 24.80. mp = 118.5−119 °C. MS (ESI) Calcd. for $C_{13}H_{23}N_2O_2^+$ ($M^+$): 239.18; Found: 239.18.

*6-(2,5-Dioxo-2H-pyrrol-1(5H)-yl)-N,N,N-trimethyl-d$_9$-hexan-1-aminium iodide (**2c-d$_9$**).* Compound **2c-d$_9$** was prepared by the same method as **2a-d$_9$** starting from **1c** and iodomethane-$d_3$. Yield: 90%. $^1$H NMR (400 MHz, $D_2O$) $\delta$ 6.88 (s, 2H), 3.55 (t, $J$ = 7.0 Hz, 2H), 3.34 (td, $J$ = 5.0 and 4.3 Hz, 2H), 1.81 (q, $J$ = 7.2 Hz, 2H), 1.63 (q, $J$ = 7.1 Hz, 2H), 1.35−1.47 (m, 4H); $^{13}$C NMR (100 MHz, $D_2O$) $\delta$ 173.43, 134.35, 66.29, 51.98, 37.44, 27.38, 25.41, 24.94, 22.12. mp 109−110 °C. MS (ESI) Calcd. for $C_{13}H_{14}D_9N_2O_2^+$ ($M^+$): 248.27; Found: 248.31.

*2-(2-(2-(2,5-Dioxo-2H-pyrrol-1(5H)-yl)ethoxy)ethoxy)-N,N,N-trimethylethanaminium iodide (**2d-d$_0$**).* Compound **2d-d$_0$** was prepared by the same method as **2a-d$_0$** starting from **1d** and iodomethane. Yield: 65%. $^1$H NMR (500 MHz, $D_2O$) $\delta$ 6.93 (s, 2H), 3.99 (tdd, $J$ = 3.0, 2.5, and 2.0 Hz, 2H), 3.70−3.80 (m, 8H), 3.62 (t, $J$ = 5.0 Hz, 2H), 3.23 (s, 9H); $^{13}$C NMR (100 MHz, $D_2O$) $\delta$ 172.97, 134.53, 69.69, 69.26, 67.76, 65.34, 64.40, 54.04, 37.10. MS (ESI) Calcd. for $C_{13}H_{23}N_2O_4^+$ ($M^+$): 271.18; Found: 271.20.

*2-(2-(2-(2,5-Dioxo-2H-pyrrol-1(5H)-yl)ethoxy)ethoxy)-N,N,N-trimethyl-d$_9$-ethanaminium iodide (**2d-d$_9$**).* Compound **2d-d$_9$** was prepared by the same method as **2a-d$_9$** starting from **1d** and iodomethane-$d_3$. Yield: 51%. $^1$H NMR (400 MHz, $D_2O$) $\delta$ 6.93 (s, 2H), 3.99 (tdd, $J$ = 2.8, 2.6, and 2.0 Hz, 2H), 3.70−3.80 (m, 8H), 3.62 (t, $J$ = 4.8 Hz, 2H); $^{13}$C NMR (100 MHz, $D_2O$) $\delta$ 172.97, 134.52, 69.67, 69.25, 67.76, 65.04, 64.36, 52.70, 37.08. MS (ESI) Calcd. for $C_{13}H_{14}D_9N_2O_4^+$ ($M^+$): 280.30; Found: 280.33.

**Preparation of Lipid Vesicles.** 100-nm diameter unilamellar vesicles (large unilamellar vesicles, LUV) were made from mixtures of lipids by extrusion. (LIPEX Extruder, Northern Lipids Inc., Vancouver, BC, Canada) The lipids were mixed in a 25-mL round-bottomed flask, dried as a thin film under reduced pressure in a rotary evaporator, and evacuated under high vacuum for 2 h. The lipid mixtures were resuspended in 50 mM sodium phosphate (pH 7.0) with vortexing and sonication. Each sample underwent five freeze−thaw cycles at −80 and 37 °C. TCEP (final concentration 100 $\mu$M) was added to reduce thiols at 25 °C, and the mixture extruded 10 times through two stacked 100-nm filters (Whatman, Newton, MA) using a $N_2$ gas pressure of 350−400 psi, to provide a homogeneous batch of unilamellar vesicles. The size of the vesicles was confirmed by dynamic light scattering (Brookhaven Instruments, DLS-90). Specific mixtures of lipids used are described below.

*Thiolipid Vesicles.* 1,2-Dipalmitoyl-*sn*-glycero-3-phosphothioethanol, PTE (sodium salt, 1.6 $\mu$mol) and 1-palmitoyl-2-oleoyl-*sn*-glycero-3-phosphocholine, POPC or 1-palmitoyl-2-palmitoyl-*sn*-glycero-3-phosphocholine, DPPC (78.4 $\mu$mol) were mixed in $CHCl_3$ (3 mL), dried, and resuspended as described above in 50 mM sodium phosphate (20 mL, pH 7.0) to yield PTE/POPC (2/98) or PTE/DPPC (2/98) vesicles.

*Peptide-Containing Vesicles.* Peptide **3** (0.5 $\mu$mol), peptide **4**, (0.5 $\mu$mol), peptide **5**, (0.5 $\mu$mol), or peptide **3**/peptide **4** (1/1, 0.32 $\mu$mol each) dissolved in ethanol (3 mL) and POPC (40 $\mu$mol) or POPC/cholesterol (30 $\mu$mol/10 $\mu$mol) in $CHCl_3$ (3 mL) were mixed, dried, and resuspended as described above in 50 mM sodium phosphate (10 mL, pH 7.0) to yield peptide **3**/POPC (1/80), peptide **4**/POPC (1/80), peptide **5**/POPC (1/80), peptide **3**/peptide **4**/POPC (1/1/127), peptide **4**/POPC/cholesterol (1/60/20), or peptide **5**/POPC/cholesterol (1/60/20) vesicles. The incorporation of peptide into the vesicles was confirmed by monitoring the fluorescence blue shift of the tryptophan emission upon excitation at 280 nm.

*Peptide and Thiolipid-Containing Vesicles.* Peptide **4** (0.5 $\mu$mol dissolved in ethanol (3 mL), PTE (0.8 $\mu$mol), and POPC or DPPC (39.2 $\mu$mol) in $CHCl_3$ (3 mL) were mixed, dried, and resuspended in 50 mM sodium phosphate (10 mL, pH 7.0) to yield peptide **4**/POPC/PTE (1/1.6/78.4), or peptide **4**/DPPC/PTE (1/1.6/78.4) vesicles. The incorporation of peptide into the vesicles was confirmed by monitoring the fluorescence blue shift of the tryptophan emission upon excitation at 280 nm.

*Vesicles with Encapsulated Carboxyfluorescein.* Peptide **4** (0.5 $\mu$mol) dissolved in ethanol (3 mL) and POPC (40 $\mu$mol) in $CHCl_3$ (3 mL) were mixed and resuspended in 50 mM sodium phosphate (5 mL, pH 7) containing 5(6)-carboxyfluorescein (0.5 mmol). LUVs were prepared as described above. Excess carboxyfluorescein was removed by size exclusion chromatography (PD-10 column, Sephadex G-25 M, GE Healthcare, Little Chalfont, Buckinghamshire, UK). POPC vesicles were prepared analogously from a solution of POPC (40 $\mu$mol) in $CHCl_3$ (3 mL).

*Vesicles with Encapsulated NB-ECD-OMe.* Peptide **4** (0.5 $\mu$mol) dissolved in ethanol (3 mL) and POPC (40 $\mu$mol) in $CHCl_3$ (3 mL) were mixed, dried, and resuspended in 50 mM sodium phosphate (5 mL, pH 7) containing NB-ECD-OMe peptide (15 $\mu$mol). LUVs were prepared as described above for vesicles with encapsulated carboxyfluorescein.

**Labeling of Peptide 3 and Peptide 4 with ICMT Probes.** Peptide **3** or peptide **4** (50 $\mu$M, 200 $\mu$L) was suspended as described above, but without lipid, in 50 mM sodium phosphate (pH 7.0, with 0.5% SDS w/v) and was reduced with TCEP (1.6 $\mu$L, 300 mM stock solution in $H_2O$, 2.5 mM final concentration) at 25 °C for 10 min. An equimolar mixture (9 mM each) of **2a-d$_0$** + **2a-d$_9$**, **2b-d$_0$** + **2b-d$_9$**, **2c-d$_0$** + **2c-d$_9$**, or **2d-d$_0$** + **2d-d$_9$** was added and the solutions were incubated at 25 °C for 1 h before analysis by MALDI-TOF mass spectrometry.

**Dye Leakage Assay.** Encapsulated-carboxyfluorescein peptide **4**/POPC (1/80) (285 $\mu$M total lipid) or POPC (285 $\mu$M total lipid) vesicles (1 mL in fluorescence cuvette) were incubated at 25 °C. Fluorescence emission intensity ($\lambda_{em}$ = 517 nm, $\lambda_{ex}$ = 492 nm) was monitored as a function of time for 75 min. After 65 min, Triton X-100 (30.9 $\mu$L, 1% w/v, stock solution in $H_2O$, 0.03% w/v, final concentration) was added, and emission intensity monitored for a further 10 min.

**Two-Step Labeling of Encapsulated NB-ECD-OMe in Peptide 4/POPC Vesicles.** Peptide **4**/POPC (1/80) vesicles containing encapsulated NB-ECD-OMe (4 mM total lipid, 200 $\mu$L) were incubated at 30 °C. Heavy probe **2a-d$_9$**, **2b-d$_9$**, **2c-d$_9$**, or **2d-d$_9$** (27.3 $\mu$L, 50 mM stock solution in $H_2O$, 6 mM final concentration) was added to the vesicles, aliquots (50 $\mu$L) were removed at 2, 30, 60, and 90 min, and added to a tube containing DTT (3.8 $\mu$L, 100 mM stock solution, 7 mM final concentration). Triton X-100 (1.7 $\mu$L, 1% w/v stock solution in $H_2O$, 0.03% w/v final concentration) was added to the solution. The solution was mixed by vortex and incubated at 25 °C for 1 h. Light probe **2a-d$_0$**, **2b-d$_0$**, **2c-d$_0$**, or **2d-d$_0$** (9.8 $\mu$L, 100 mM stock solution in $H_2O$, 15 mM final concentration) was added to the solution and the solution was incubated at 25 °C for 1 h before analysis by LC/MS on an Agilent, Kinetex C18 column (2.6 $\mu$m, 100 Å, 100 × 2 mm); solvent A: $H_2O$ (0.1% TFA), solvent B: ACN (0.1% TFA); $T$ = 35 °C; 0.6 mL/min; t = 0−1′, B = 3%, t = 1−16′, B = 3−49%. The integrated areas for both heavy and light peptides are derived from extraction of these masses from total ion counts. The percentage heavy label was calculated as integrated area of heavy labeled peptide/(integrated area of light labeled peptide + integrated area of heavy labeled peptide). The percentage of heavy label present at 2 min was subtracted from each time point to correct for extra vesicular NB-ECD-OMe peptide remaining from the vesicle preparation.

**Two-Step Labeling of Peptide 3 in POPC Vesicles.** Heavy probe **2a-d$_9$**, **2b-d$_9$**, **2c-d$_9$**, or **2d-d$_9$** (10 $\mu$L, 100 mM stock solution in $H_2O$, 9 mM final concentration) was added to peptide **3**/POPC (1/80) vesicles (4 mM total lipid, 100 $\mu$L), and the mixture was incubated at 30 °C for 1 h. DTT (11 $\mu$L, 100 mM stock solution, 10 mM final concentration) and sodium cholate (6.3 $\mu$L, 20% w/v, stock solution in $H_2O$, 0.5% w/v, final concentration) were added to the solution. The solution was mixed by vortex and incubated at 25 °C for 1 h. Light probe **2a-d$_0$**, **2b-d$_0$**, **2c-d$_0$**, or **2d-d$_0$** (84 $\mu$L, 100 mM stock solution in $H_2O$, 25 mM final concentration) was added to the solution and the solution was incubated at 75 °C for 1 h before analysis by MALDI-TOF mass spectrometry.

**Two-Step Labeling of Peptide 4 in POPC Vesicles.** Heavy probe **2a-d$_9$**, **2b-d$_9$**, **2c-d$_9$**, or **2d-d$_9$** (2.5 $\mu$L, 20 mM stock solution in $H_2O$, 500 $\mu$M final concentration) was added to peptide **4**/POPC (1/80) vesicles (4 mM total lipid, 100 $\mu$L), and the mixture was incubated at 30 °C for 1 h. DTT (8.3 $\mu$L, 20 mM stock solution in $H_2O$, 1.5 mM final solution) and Triton X-100 (3.43 $\mu$L, 1% w/v, stock solution in $H_2O$, 0.03% w/v, final concentration) were added to the solution. The solution was mixed by vortex and incubated at 25 °C for 1 h. Light probe **2a-d$_0$**, **2b-d$_0$**, **2c-d$_0$**, or **2d-d$_0$** (18 $\mu$L, 100 mM stock solution in $H_2O$, 13.6 mM final concentration) was added to the solution and the solution was incubated at 25 °C for 1 h before analysis by MALDI-TOF mass spectrometry.

**Kinetics of Labeling Peptides in Vesicles.** Peptide **4**/POPC (1/80) vesicles (4 mM total lipid, 100 $\mu$L) were incubated at 30 °C for 5 min and then heavy probe **2a-d$_9$** or **2c-d$_9$** (5 $\mu$L, 2.5 mM stock solution in $H_2O$, 125 $\mu$M final concentration) was added to the solution. After 2, 5, 10, 30, 60, or 120 s, light probe **2a-d$_0$** or **2c-d$_0$** (26.25 $\mu$L, 5 mM stock solution in $H_2O$, 1.25 mM final concentration) was added to the solution. Then the solution was incubated at 25 °C for 5 min. Next, DTT (6.5 $\mu$L, 100 mM stock solution in $H_2O$, 4.5 mM final concentration) and Triton X-100 (4.3 $\mu$L, 1% w/v, stock solution in $H_2O$, 0.03% w/v, final concentration) were added, the solution was mixed by vortex, and incubated at 25 °C for 5 min before analysis by MALDI-TOF mass spectrometry. Kinetic labeling of peptide **4**/POPC/cholesterol (1/60/20), peptide **5**/POPC (1/80), peptide **5**/POPC/cholesterol (1/60/20), peptide **4**/POPC/PTE (1/1.6/78.4), or peptide **4**/DPPC/PTE (1/1.6/78.4) vesicles was performed following the same procedure.

In the case of peptide **3**/peptide **4**/POPC (1/1/127) vesicles, 5 mM total lipid (100 $\mu$L) was used, and after the second labeling step, one sample (**2a-d$_9$**/**2a-d$_0$**) was incubated for another 5 min at 30 °C, then vesicles were lysed with sodium cholate (1.75 $\mu$L, 20% w/v, stock solution in $H_2O$, 0.5% w/v final concentration), and an additional aliquot of **2a-d$_0$** (20 $\mu$L, 100 mM stock solution in $H_2O$, 27 mM final concentration) was added to the mixture that was incubated at 25 °C for 1 h before analysis by MALDI-TOF mass spectrometry. Cholate is required for labeling peptide **3** in detergent micelles after vesicle lysis.

In the case of peptide **4**/PTE/POPC (1/1.6/78.4) or peptide **4**/PTE/DPPC (1/1.6/78.4), vesicles were incubated at 30 °C for 5 min and heavy probe **2a-d$_9$** (10 $\mu$L, 5 mM stock solution in $H_2O$, 455 $\mu$M final concentration) was added to the solution. After 2, 5, 10, 30, 60, 120, 300, 600, or 900 s, light probe **2a-d$_0$** (32.4 $\mu$L, 20 mM stock solution in $H_2O$, 4.55 mM final concentration) was added to the solution that was incubated at 25 °C for 5 min. Then Triton X-100 (4.4 $\mu$L, 1% w/v, stock solution in $H_2O$, 0.03% w/v, final concentration) was added, mixed by vortex, and the mixture was incubated at 25 °C for 5 min. DTT (11 $\mu$L, 100 mM stock solution in $H_2O$, 7 mM final concentration) was added, and the mixture was incubated at 25 °C for 5 min before analysis by MALDI-TOF mass spectrometry.

**Two-Step Labeling of Thiolipid Vesicles with ICMT Probe.** PTE/POPC (2/98) or PTE/DPPC (2/98) vesicles (4 mM total lipid, 850 $\mu$L) were incubated at 30 °C for 5 min, heavy probe **2a-d$_9$** (10.8 $\mu$L, 20 mM stock solution in $H_2O$, 250 $\mu$M final concentration) was added to the vesicles, aliquots (100 $\mu$L) were removed at 1, 2, 5, 10, 15, 20, 30, and 90 min, and added to a tube containing DTT (11 $\mu$L, 20 mM stock solution in $H_2O$, 2 mM final concentration). Triton X-100 (3.4 $\mu$L, 1% w/v stock solution in $H_2O$, 0.03% w/v final concentration) was added to the solution. The solution was mixed by vortex and incubated at 25 °C for 5 min. Light probe **2a-d$_0$** was added (28.6 $\mu$L, 50 mM stock solution in $H_2O$, 10 mM final concentration) and the solution was incubated at 25 °C for 1 h before analysis by MALDI-TOF mass spectrometry. The kinetics of PTE flipping between bilayers were sufficiently slow that this original two-step labeling procedure with a quench step in between addition of the first and second probe could be used.

**Sample Preparation for MALDI Analysis.** The matrices were prepared by dissolving $\alpha$-cyano-4-hydroxycinnamic acid (CHCA, 20 mg/mL) in a 3/7 (v/v) mixture of 5% (v/v) formic acid in $H_2O$/ACN, 2,5-dihydroxybenzoic acid (DHB, 20 mg/mL) in a 3/7 (v/v) mixture of 0.1% TFA (v/v) in $H_2O$/ACN, or sinapinic acid (SA, 20 mg/mL) in a 3/7 (v/v) mixture of 0.1% TFA (v/v) in $H_2O$/ACN. A MTP 384 target plate (Bruker Daltonic, Billerica, MA) was used for MALDI analysis. Prior to application to the sample plate, the labeled peptide sample solutions were mixed with matrix in a 1:1−1:3 ratio (v/v). The sample−matrix mixture (1 $\mu$L) was applied onto the MTP384 target plate and was allowed to air-dry before acquiring mass spectra.

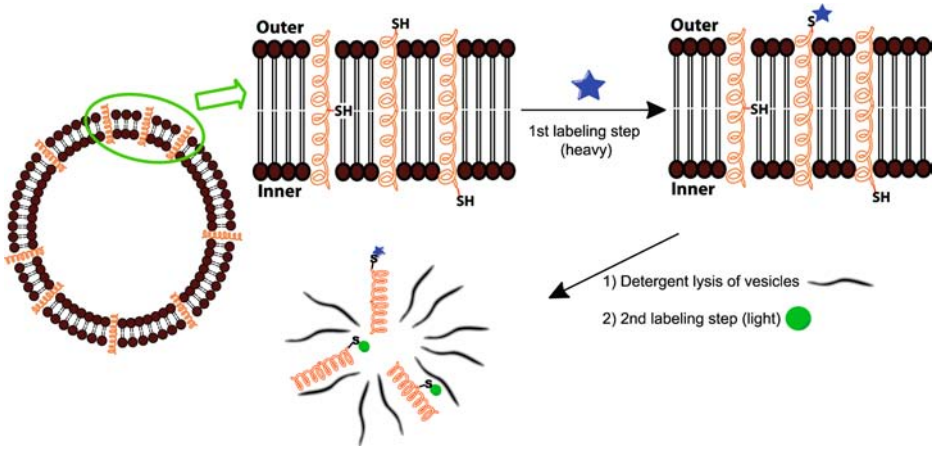


**Figure 3.** Labeling strategy for transmembrane $\alpha$-helical peptides incorporated into POPC vesicles. The cysteine is in a solvent inaccessible or accessible position for peptides **3** or **4**, respectively. In the case of peptide **4**, only the thiol on the outer leaflet is exposed to ICMT probe. The cysteine was first labeled with heavy probe in intact vesicles; the vesicles were lysed with detergent, and then labeled with light probe.

**Mass Spectrometry.** Spectra were acquired on a Bruker Autoflex II MALDI-TOF/TOF mass spectrometer (Bruker Daltonic, Billerica, MA), operated in the reflectron mode. A nitrogen laser UV laser (337 nm, 1−5 ns pulse of max energy 140 $\mu$J, 10 Hz) was used to accomplish desorption/ionization. The positive ions were subjected to an accelerating potential of 19.0 kV and 16.9 kV from ion source 1 and ion source 2, respectively, 8.35 kV for the optical lens, reflected by reflectron electrodes (20 kV and 9.52 kV), and detected by a microchannel plate (MCP) detector using 4× voltage gain. The pulsed ion extraction time was 135 ns. Matrix ions were suppressed using a low mass ($m/z$ 500) cutoff. The raw mass spectra were analyzed by Bruker flexAnalysis version 3.0 software.

## RESULTS

**Synthesis of ICMT Labeling Reagents.** The ICMT reagents were prepared in excellent yields from the protected aminoalkyl maleimides **13a−13d**, which in turn were obtained from maleic anhydride and diamines (Figure 2). Quantitative deprotection of the terminal amines **13a−13d** (Figure 2) and subsequent permethylation[17] with iodomethane provided the quaternary ammonium salts **2a-$d_0$−2d-$d_0$** in high purity (Figure 1). Analogously, permethylation with iodomethane-$d_3$ provided the heavy isotope forms **2a-$d_9$−2d-$d_9$**.

**Design of Transmembrane Peptides for Assessment of Membrane Access.** We prepared three model transmembrane peptides each with a single cysteine to assess the reactivity of our probes with peptide thiols in lipid membranes. The peptide sequence Ac-$K_2GL_9WL_9K_2A$-$NH_2$ forms an $\alpha$-helix and spans the lipid bilayer.[18] This peptide and peptides with related sequences have been used widely to study membrane structure with fluorescence and EPR probes.[18] The tryptophan fluorescence emission reports on the incorporation and orientation of peptide in the membrane, and a blue shift in tryptophan emission from 350 to 316 nm signifies that the transmembrane conformation has been adopted. We introduced a cysteine residue in the middle of the sequence to provide peptide **3** (Ac-$K_2GL_7WLCL_9K_2A$-$NH_2$), incorporated a cysteine at the N-terminus to provide peptide **4** (Ac-$CK_2GL_7WLAL_9K_2A$-$NH_2$), and placed a cysteine after the two lysines at the N-terminus to provide peptide **5** (Ac-$K_2CL_7WLAL_9K_2A$-$NH_2$) (Figure S1). We expected the central cysteine in peptide **3**, which is buried in the membrane, would be inaccessible to our maleimide probes. Conversely, for that population of peptide **4** oriented with the terminal cysteine thiol protruding from the outer leaflet, we expected the thiol to be accessible to the probes. Peptide **5** was designed to place the cysteine in a position partially accessible to probe as the thiol is expected to reside at the boundary between the lipid headgroup region and hydrophobic core of the membrane.

**Assessment of ICMT Labeling Precision and Accuracy.** To test the accuracy and repeatability of mass spectral peak integration, we labeled peptide **3** or peptide **4** that had been suspended in 5% aqueous detergent solution with a 1:1 (molar) mixture of heavy and light probes. The experimental percentage of heavy and light labeling was determined two different ways using Bruker flexAnalysis version 3.0 software. First, the average intensities of the heavy and light isotopomers were measured. Second, the areas under the entire heavy and light isotopic envelopes were measured. The percentage of heavy-labeled peptide was calculated from both sets of values. As shown in Figure S2, the ratio of labeling by heavy and light labels was close to 1:1. There was only a few percent variability (generally 2−3%) in the percent heavy-labeled peptide using either method. The detection of light and heavy labels in the expected 1:1 ratio implies that there are no detectable isotope effects on either labeling rate or ionization efficiencies.

**Membrane Permeability of ICMT Reagents.** We performed a fluorescent dye leakage assay to test membrane permeability in the presence or absence of transmembrane peptides. We prepared POPC and peptide **4**/POPC vesicles with carboxyfluorescein encapsulated, and fluorescence intensity was monitored as a function of time. The fluorescence intensity for both POPC and peptide **4**/POPC vesicle solutions remained low and unchanged over 65 min. No significant dye leakage was observed until we added Triton X-100 to disrupt lipid vesicles (Figure S3). This important control demonstrates that incorporation of transmembrane peptides does not increase the permeability of the membrane to anionic molecules.

Because of the possibility that membrane permeation may be dependent on charge, we performed an additional experiment to test directly whether the cationic nature of the probe enables it to permeate the membrane. The modified tripeptide, NB-ECD-OMe, which contains a reactive thiol, was encapsulated in

peptide **4**/POPC (1/80) vesicles. The tripeptide contains two acidic residues that are anions at neutral pH. As demonstrated for carboxyfluorescein, the anionic tripeptide is not expected to leak out of the vesicles.

We utilized a two-step labeling method as outlined in Figure 3. In the first step, the vesicles were labeled with the heavy isotope probe **2a-d$_9$**−**2d-d$_9$**. After a period of time (2−90 min), the probe was quenched with DTT, and then the vesicles were lysed with the detergent Triton X-100 and treated with light probe. If the ICMT probes were to permeate the lipid bilayer, the encapsulated NB-ECD-OMe peptide would be labeled with heavy probe during the first labeling step.

Compared to phospholipid, the quantity of NB-ECD-OMe peptide in this experiment is quite small and difficult to detect by MALDI-TOF spectrometry. Therefore, we used LC/MS to separate NB-ECD-OMe peptide from lipid and to analyze the percentage of heavy labeled peptide as a function of time. In each experiment, we observed a small amount of heavy labeled NB-ECD-OMe at the initial time point (2 min). Furthermore, we did not observe any increased labeling of the NB-ECD-OMe peptide with heavy probe over the course of 90 min (Figure S4). Almost all labeling was with the light probe, indicating that encapsulated NB-ECD-OMe was only accessible to label after the membranes were solubilized. The small amount of heavy labeled NB-ECD-OMe is probably due to a trace of peptide that remains outside the vesicles after size exclusion chromatography. These data confirm the impermeability of the transmembrane-containing lipid bilayer to the ICMT probes (Figure S4).

**ICMT Detection of Peptide Thiol Membrane Location.** We prepared POPC vesicles with 1.25 mol percent of peptide **3** or peptide **4**. Each vesicle type was subjected independently to labeling with each of the ICMT heavy/light probe sets. We utilized a two-step labeling method similar to that used for the NB-ECD-OMe peptide, as outlined in Figure 3. In the first step, the vesicles were labeled with the heavy isotope probe. After 10 min, the probe was quenched with DTT, and then the vesicles were lysed with Triton X-100, and then treated with light probe. Because all four of the ICMT probes did not permeate the membrane, we expected that only thiols on the outer leaflet exposed to the aqueous environment would be labeled in the first step. Analogously, we expected that thiols buried in the membrane or with thiol exposed on the inner surface would be labeled after disruption of the lipid bilayers. We analyzed the heavy/light labeling percentage by integrating the full isotopic envelope as described above.

We found that neither heavy nor light ICMT probe labeled peptide **3** under these conditions. We postulated that the thiol in peptide **3** was too deeply buried in a hydrophobic environment to react with ICMT probe both in the vesicles and in the detergent micelles formed upon lysis of the membrane vesicles with Triton X-100 detergent. Therefore, we employed sodium cholate, which has a higher CMC and forms smaller micelles unlikely to deeply bury the thiol group of Cys,[19] to disrupt the vesicles, and also used elevated temperature to increase the labeling reaction rate. Under these conditions, the thiol of peptide **3** is labeled efficiently in the second step (Figure 4A−D), consistent with our hypothesis.

In the case of peptide **4**, we found that the solvent accessible cysteine was readily labeled in the first step. However, with most of the ICMT probes, 100% of the cysteine in peptide **4** was labeled in the first step, rather than the 50% expected if the

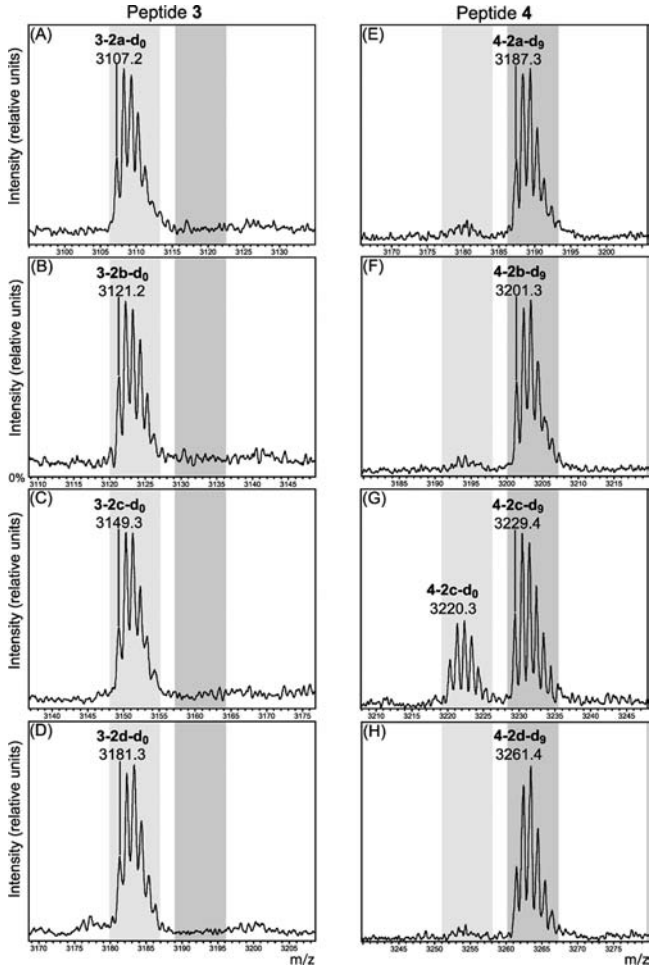


**Figure 4.** Mass spectra of peptide **3** and peptide **4** in POPC vesicles labeled in the two-step procedure outlined in Figure 3. Peptide/POPC vesicles were labeled with heavy probe for one hour in the first step, lysed with detergent, and then labeled with light probe for one hour. Peptide **3** labeled with heavy/light probes (A) **2a-d$_9$**/**2a-d$_0$**, (B) **2b-d$_9$**/**2b-d$_0$**, (C) **2c-d$_9$**/**2c-d$_0$**, or (D) **2d-d$_9$**/**2d-d$_0$**; and peptide **4** labeled with heavy/light probes (E) **2a-d$_9$**/**2a-d$_0$**, (F) **2b-d$_9$**/**2b-d$_0$**, (G) **2c-d$_9$**/**2c-d$_0$**, or (H) **2d-d$_9$**/**2d-d$_0$**. Peptide **3**/POPC vesicles were lysed with 0.5% (w/v) sodium cholate at 25 °C and labeled with light probe at 75 °C. Peptide **4**/POPC vesicles were lysed with 0.03% (w/v) Triton X-100 and labeled with light probe at 25 °C. The peaks corresponding to light-labeled peptide are highlighted in light gray, and the peaks corresponding to heavy-labeled peptide are highlighted in dark gray. Intensities are relative to the highest peak in a single spectrum and each panel is not on the same scale.

peptides were randomly oriented so that half of the thiol population is oriented toward the center of the vesicle and the other half faces the external solution (Figure 4E−H). When we examined the kinetics of labeling peptide **4**, we found that within one minute over 90% of the thiol was labeled in the first step regardless of ICMT probe concentration. Previous work had identified a population of the $\alpha$-helical peptide that orients parallel to the surface rather than in a transmembrane orientation, and found that equilibration between the two states is rapid.[20,21] Our data suggest that, upon transitioning between the transmembrane and parallel orientations, the thiol orientation can invert from outer to inner leaflet and vice versa. If the time scale of this peptide flip is faster than the labeling time, then all of the solvent accessible thiol would be labeled in a single, fast step.


dx.doi.org/10.1021/bc400171j | *Bioconjugate Chem.* 2013, 24, 1235−1247

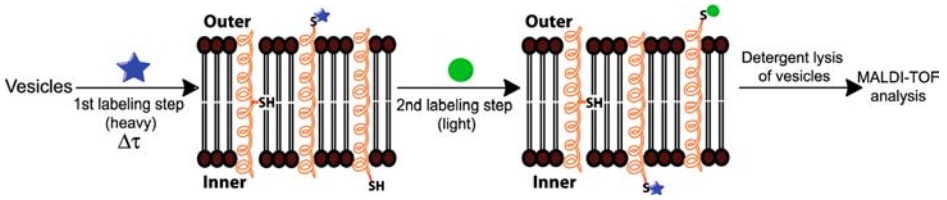


**Figure 5.** Schematic illustration of kinetic labeling strategy for transmembrane $\alpha$-helical peptides incorporated into POPC vesicles. The cysteine is in a solvent inaccessible or accessible position for peptides **3** or **4**, respectively. Peptide **3**/peptide **4**/POPC was first labeled with heavy probe, and 2, 5, 10, 30, 60, or 120 s after adding the first probe, a 10-fold excess of light probe was added.

**ICMT Monitoring of Peptide Helix Mobility Kinetics in Membranes.** To assess whether peptide flipping in lipid membranes is occurring on the second time scale, we revised our labeling scheme and performed kinetics experiments (Figure 5). Peptide **4**/POPC vesicles (1/80) were labeled with **2a-d$_9$** or **2c-d$_9$** for 2 to 120 s, then a 10-fold excess of **2a-d$_0$** or **2c-d$_0$** was added for five minutes before lysing vesicles for analysis. The amount of labeling observed in the first step increased with time and thiol labeling was complete within thirty seconds (Figure S5). The reaction rates were nearly identical for the two linkers tested.

Next, we incorporated both peptide **3** and peptide **4** into the same POPC vesicle in order to assess the efficacy of labeling thiols in two different environments in a single membrane bilayer. The kinetic time courses for these mixtures of peptides labeled with **2a-d$_9$**/**2a-d$_0$** or **2c-d$_9$**/**2c-d$_0$** (Figure 6) were identical to the time courses for the peptides incorporated into individual membranes (Figure S5). Again, peptide **3** containing the inaccessible peptide was not labeled until the vesicles were lysed. In contrast, positioning the peptide cysteine two residues from the N-terminus, i.e., peptide **5**, slowed, but did not block thiol labeling (Figure 8B). This small shift in thiol position in the peptide sequence resulted in an approximately 5-fold reduction in labeling rate.

We also reversed the order of probe addition. We initially labeled with the light probe **2a-d$_0$**, and added an excess of heavy probe **2a-d$_9$** as a function of time (Figure 7). Within experimental error, the rate of labeling in the first step was independent of which isotope or probe was used (compare Figure 7B to Figure 6B). From the combined results of these experiments we conclude that the flipping of peptide orientation is occurring within seconds. This is only an upper limit to the time required for flipping.

**Membranes Can Regulate Accessibility to Cysteine.** To further investigate the effects of different lipid membrane compositions on peptide dynamics, we utilized the same kinetic labeling scheme outlined in Figure 5 with peptide **4**/POPC/cholesterol (1/60/20) lipid vesicles and probe **2a**. The introduction of cholesterol reduced both the initial rate of labeling, as well as the peptide flip rate (Figure 8A, Table 1). The labeling rate was reduced about 4-fold. Moreover, a population of peptide remained inaccessible to probe when cholesterol was included in the lipid bilayer.

When the same comparison was performed with peptide **5**, a similar 4-fold reduction in the rate of peptide labeling in the presence of cholesterol was observed (Figure 8B, Table 1). Therefore the relative changes in peptide labeling and flipping rates are independent of the position of thiol and are a consequence of lipid composition (see Discussion) that influences bilayer structure.

**ICMT Monitoring of Lipid and Peptide Flip Rate in Fluid and Gel State Membranes.** We further tested the

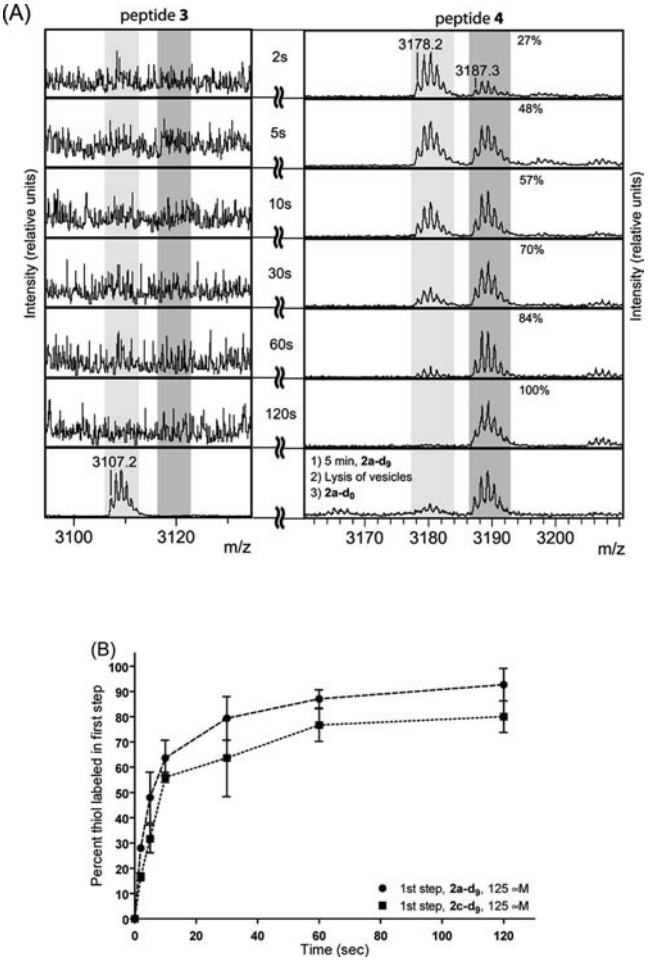


**Figure 6.** Kinetics of labeling peptide **3**/peptide **4**/POPC vesicles (1/1/127). The vesicles were first labeled with 125 $\mu$M **2a-d$_9$** or **2c-d$_9$**, and 2, 5, 10, 30, 60, or 120 s after adding the first probe, 1.25 mM **2a-d$_0$** or **2c-d$_0$**, respectively, was added. (A) Mass spectra of peptide **3** (left) and peptide **4** (right) labeled with **2a-d$_9$**/**2a-d$_0$** at different time points. Bottom panel: after labeling 5 min with **2a-d$_9$**, the vesicles were lysed (cholate, 75 °C) and a 300-fold excess of light probe, **2a-d$_0$**, was added. Intensities are relative to the highest peak in a single spectrum and each panel is not on the same scale. (B) Time courses for peptide **4** labeling for the two probes, **2a** and **2c**. Integrated areas under the isotopic envelope were used to calculate percent labeling.

ability of the ICMT probes to detect membrane dynamics using unilamellar vesicles that contain a synthetic lipid 1,2-dipalmitoyl-*sn*-glycero-3-phosphothioethanol (PTE). This lipid includes a terminal thiol in the headgroup in place of the amino group typically found in phosphatidylethanolamine (PE). Although phospholipids can move from the outer leaflet to the inner leaflet and vice versa, the transverse diffusion rate is

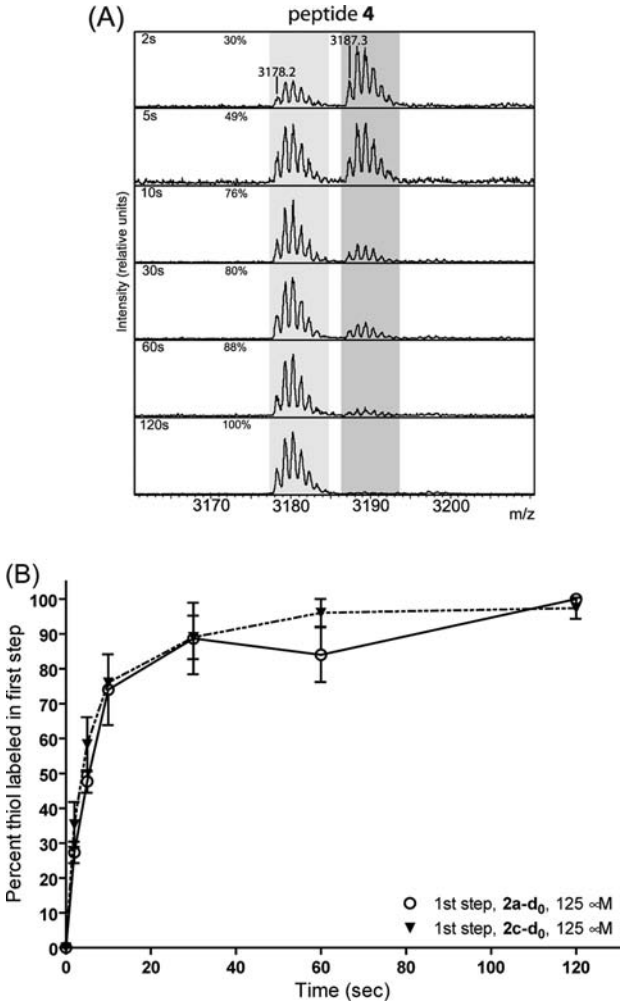


**Figure 7.** Kinetics of reversed order of probe addition on labeling peptide **3**/peptide **4**/POPC vesicles (1/1/127). The vesicles were first labeled with 125 $\mu$M **2a-d$_0$** or **2c-d$_0$**, and 2, 5, 10, 30, 60, or 120 s after adding the first probe, 1.25 mM **2a-d$_9$** or **2c-d$_9$**, respectively, was added. (A) Mass spectra of peptide **4** labeled with **2a-d$_0$**/**2a-d$_9$** at different time points. Intensities are relative to the highest peak in a single spectrum and each panel is not on the same scale. (B) Time courses for the two labeling experiments. Integrated areas under the isotopic envelope were used to calculate percent labeling in the first step for peptide **4**.

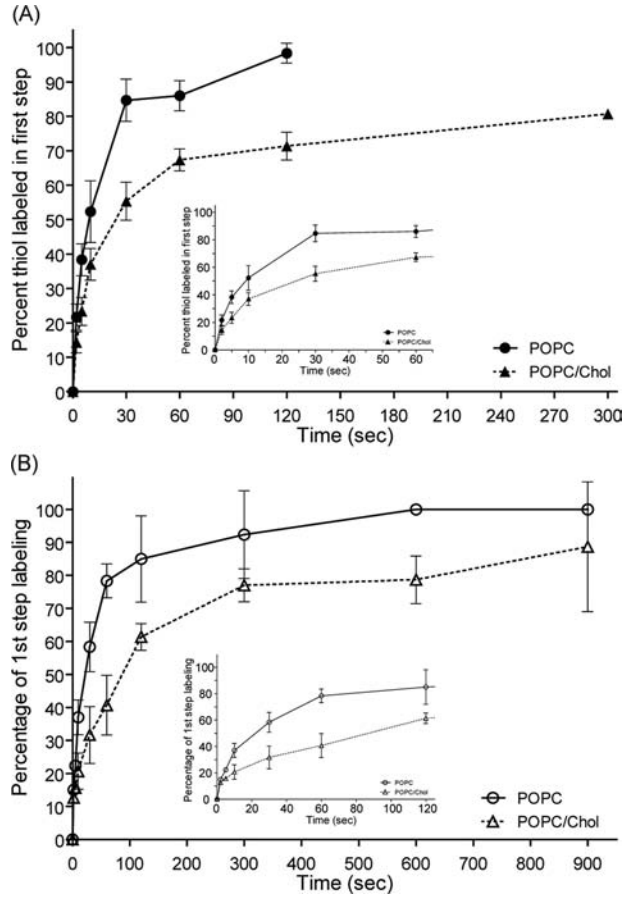


**Figure 8.** Kinetics of labeling peptide **4** and peptide **5** in POPC or POPC/cholesterol vesicles (3/1). The vesicles were first labeled with 125 $\mu$M (250 $\mu$M for peptide **5**/POPC and peptide **5**/POPC/cholesterol vesicles) **2a-d$_9$**, and 2, 5, 10, 30, 60, 120, 300, 600, or 900 s after adding the first probe, 1.25 mM (2.5 mM for peptide **5**/POPC and peptide **5**/POPC/cholesterol vesicles) **2a-d$_0$** was added. (A) Time courses for labeling peptide **4** in POPC or POPC/cholesterol (3/1) vesicles. Integrated areas under the isotopic envelope were used to calculate percent labeling. Inserted figure is a magnification of the first 60 s. (B) Time courses for labeling peptide **5** in POPC or POPC/cholesterol (3/1) vesicles. Integrated areas under the isotopic envelope were used to calculate percent labeling. Inserted figure is a magnification of the first 120 s.

usually on the order of hours to days.[22] Thus, on the time scale of our labeling experiment, which is minutes, the thiolipid PTE should not exchange between leaflets, and assuming that in the vesicles, the PTE is randomly distributed between the inner monolayer (which has about 45% of the total lipid in 1000 Å vesicles) and outer monolayer (which has about 55% of the lipid in 1000 Å vesicles), we expected that only 55% of the thiolipid would be labeled in intact vesicles, i.e., in the first labeling step, although introduction of transmembrane peptide or alteration of lipid composition can accelerate flopping rate in membranes.[23,24]

We prepared PTE/POPC (2/98), peptide **4**/PTE/POPC (1/1.6/78.4), PTE/DPPC (2/98), and peptide **4**/PTE/DPPC (1/1.6/78.4) vesicles, and performed two-step labeling of thiolipid and peptide **4**. We compared the rates of thiolipid and peptide **4** labeling (Figure 9). We found that the rate of thiolipid labeling was about 100−150-fold slower than peptide **4** labeling, suggesting that the physical environment around the thiol of the PTE is quite different from that of peptide. It is possible that the PTE p$K_a$ is elevated due to its proximity to the phosphate group.

The initial rate of PTE labeling was reduced 2−3-fold upon changing the lipid composition from one that forms the liquid phase (POPC) to one that forms gel phase (DPPC) (Figure 9B and D), consistent with tighter packing of head groups in the gel phase. Introduction of 1.3 mol percent peptide into the lipid bilayer increased the outer lipid labeling rate more than 7-fold. In the case of POPC membranes, the lipid flip rate also increased in the presence of peptide **4**. The change in flip rate can be attributed to decreased order in the bilayer structure upon addition of peptide. This effect was observed previously by de Kruijff and co-workers.[23,24] This change may also reflect an increase in the amount of the reactive anionic thiolate in the presence of the peptide (which is cationic), or an increase in thiol exposure to aqueous solution in the presence of the peptide.


dx.doi.org/10.1021/bc400171j | Bioconjugate Chem. 2013, 24, 1235−1247

**Table 1. Relative Rate of Transmembrane Peptide Labeling in Different Lipid Compositions**[a]

| peptide/lipid | time to label 50% (s) | [**2a-d$_9$**] ($\mu$M) | $1/t_{50}$x[probe] $M^{-1}$ $s^{-1}$ |
|---|---|---|---|
| Peptide **4**/POPC | 9 | 125 | 889 |
| Peptide **4**/POPC/ Cholesterol | 25 | 125 | 320 |
| Peptide **5**/POPC | 22 | 250 | 182 |
| Peptide **5**/POPC/ Cholesterol | 90 | 250 | 44 |
| Peptide **4**/POPC | 2.7 | 455 | 814 |
| Peptide **4**/POPC/PTE | 3.8 | 455 | 578 |
| Peptide **4**/DPPC | 25 | 455 | 88 |
| Peptide **4**/DPPC/PTE | 28 | 455 | 78 |

[a]Time to label 50% thiol on peptide in different lipid compositions at different probe concentrations is reported. The reciprocal of the time to label 50% of thiol mutiplied by probe concentration used in the first labeling step is calculated. This value should be proportional to the average rate constant over the first 50% of the reaction.

Interestingly, despite the fast initial rate of PTE labeling, the extent of labeling after 1 h was much lower than that of peptide, confirming that the flipping of PTE between leaflets was slower than that of peptide **4** or peptide **5**. In POPC vesicles, there does seem to be an appreciable rate of PTE flip, as shown by the slow increase in reaction over 1 h and the observation that the level of labeling was greater than the 55% expected in the absence of lipid flipping, while in DPPC vesicles, which are in the gel state at 25 °C, PTE flip over hours appears to be negligible. The fact that the final level of PTE labeling was only 40% in DPPC may reflect a nonrandom distribution of PTE in the inner and outer leaflet.

In contrast, to the effect of peptide on lipid labeling, the introduction of 2 mol % thiolipid did not affect the rate of peptide **4** labeling in either POPC or DPPC vesicles (Figure 9A and C, Table 1). On the other hand, there was an effect of lipid physical state upon peptide labeling. We observed that incorporation of peptide **4** into gel phase DPPC reduced the initial rate of peptide labeling at least 10-fold. Moreover, the time to 100% labeling is approximately 30-fold longer. Complete labeling is dependent on both label rate and peptide flip rate. Taken together it appears that the peptide flip rate is about three times slower in the gel phase than the liquid phase. The decrease in labeling rate may again reflect a decrease in Cys exposure to aqueous solution (see Discussion).

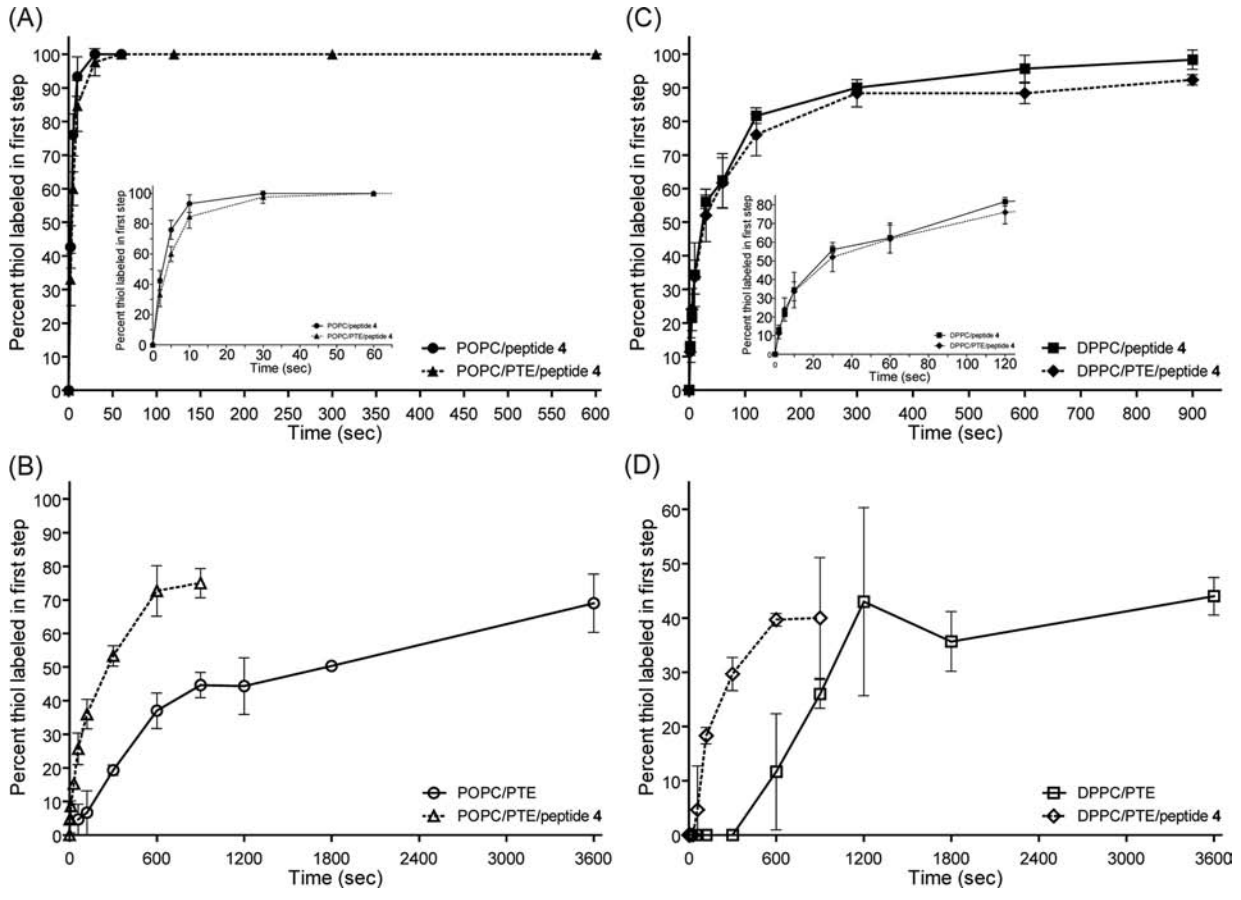


**Figure 9.** Kinetics of labeling peptide **4**/POPC (1/80), peptide **4**/PTE/POPC (1/1.6/78.4), PTE/POPC (2/98), peptide **4**/DPPC (1/80), and peptide **4**/PTE/DPPC (1/1.6/78.4), and PTE/DPPC (2/98) vesicles. The vesicles containing peptide **4** were first labeled with 455 $\mu$M **2a-d$_9$**, and 2, 5, 10, 30, 60, 120, 300, 600, or 900 s after adding the first probe, 4.55 mM **2a-d$_0$** was added. In samples in which PTE labeling was assayed in the absence of peptide, labeling was carried out with 250 $\mu$M **2a-d$_9$** heavy probe for 1, 2, 5, 10, 15, 20, 30, and 60 min, quenched by 2 mM DTT, 0.03% Triton X-100 to lyse vesicles, and were labeled with 10 mM **2a-d$_0$** light probe for 1 h. (A) Time course for labeling peptide **4** in POPC or PTE/POPC vesicles. Inserted figure is a magnification of the first 60 s. (B) Time course for labeling thiolipid, PTE, in POPC or peptide **4**/POPC vesicles. (C) Time course for labeling peptide **4** in DPPC or PTE/DPPC vesicles. Inserted figure is a magnification of the first 120 s. (D) Time course for labeling of thiolipid, PTE, in DPPC or peptide **4**/DPPC vesicles.


dx.doi.org/10.1021/bc400171j | *Bioconjugate Chem.* 2013, 24, 1235−1247

## DISCUSSION

Isotope-coded tag methods provide facile relative quantitation in mass spectrometry.[25] The originally introduced ICAT tags include a thiol reactive iodoacetyl group, a biotin for purification, and a polyether linker. The polyether linker can be labeled with 8 deuterons for isotope coding. Related labeling methods which utilize a combination of isotope tag, cysteine labeling, and mass spectrometry include acid-labile isotope-coded extractants (ALICE)[26] and isotopic tandem orthogonal proteolysis-activity-based protein profiling (isoTOP-ABPP).[27] In ALICE, cysteine-containing peptides or proteins are captured on a maleimide resin. In isotope-ABPP, the differential reactivity of cysteines is elucidated. In each of these methods, two different samples are labeled, one with light isotope and one with heavy isotope. Then, the samples are mixed and the ratio of heavy to light product is analyzed by mass spectrometry. Thus, cysteine-directed isotope-coded tags can fulfill a variety of needs in proteomic research.

Here, we have designed and synthesized a series of *N*-alkyl(alkoxy)maleimides, **2a-$d_0$**−**2d-$d_9$**, to probe protein topologies in the presence of membranes. These probes comprise three components, a thiol-reactive maleimide, a positively charged quaternary ammonium group, and linkers of varying lengths between them. We focused on a cysteine labeling method because the amino acid functionality to be tagged, in this case a thiol, can reside in the membrane with little energetic penalty. Although lysine labeling has been used widely to map surface accessibility, due to lysine's cationic charge at physiologic pHs, it is not suitable for membrane studies. We utilized a covalent labeling strategy to avoid the problem of back exchange that is a limitation of hydrogen−deuterium exchange methods. The maleimide moiety reacts specifically with sulfhydryl groups, and in a physiological pH range, it reacts faster than other thiol-targeted reagents, e.g., iodoacetamide.[28] Lastly, we developed the method such that a bottom-up analysis approach, in which the tagged protein is proteolytically reduced to smaller peptide fragments, could be employed. This approach enables monitoring of the accessibility of several sites in a single protein simultaneously. Due to isotope effects on retention times,[29] LC/MS methods require postprocessing alignment of spectra before evaluation of labeling ratios. Therefore, we chose to analyze tagged peptides with MALDI-TOF mass spectrometry in order to simplify the ratio analysis.

We incorporated a quaternary ammonium mass tag for two reasons. First, the quaternary ammonium bears a positive charge regardless of the ionization conditions in the mass spectrometer. This tag eliminates the requirement for inclusion of basic amino acids in the peptide to be analyzed.[30−32] Second, isotope incorporation is accomplished through per-methylation of a primary amine to form the quaternary ammonium in the last synthetic step. This reaction sequence provides an economical and efficient synthesis for heavy isotope incorporation. Iodomethane labeled with either $^{2}H$ or $^{13}C$ is commercially available. After per-methylation of amine, the $^{2}H$ and $^{13}C$ labels provide probes with 9 or 3 Da mass differences, respectively. Deuterium has two advantages: lower cost, and complete separation of isotopic envelopes in the mass spectra. The hydrogen and deuterium probes were easily prepared in >99% purity and multigram quantities.

We tested various lengths of carbon linker and a PEG linker to tune the membrane permeability and surface thiol reactivity of our probes. We sought a linker that both limited probe solubility in the membrane and prevented interference of the quaternary ammonium mass tag with the thiol-labeling reaction. Permeability experiments with an encapsulated peptide confirmed that all the ICMT probes were membrane impermeable over at least a 90-min period. This was true even in the presence of transmembrane peptides. Moreover, the rates of labeling were minimally affected by linker length. Therefore, all the ICMT probes are suitable to provide information on the position and dynamics of peptides in membranes. However, probe **2c** provided the least consistent labeling rates and efficiencies (Figures S2 and 6B) of all the probes, perhaps due to its higher chain flexibility and greater hydrophobicity.

We selected three peptides to model possible cysteine topologies in a protein. The sequences of these peptides were identical except for the position of the cysteine residue. The peptide sequence was selected for its ability to form a transmembrane $\alpha$-helix, and thus to position the cysteine in a midbilayer environment in the case of peptide **3**, in a lipid headgroup environment in the case of peptide **4**, or at the boundary of the lipid headgroup and the hydrocarbon region in the case of peptide **5**. Labeling was found to be very sensitive to the location of the Cys residue. Even the small difference in membrane depth for the Cys in peptide **4** and peptide **5** was sufficient to significantly slow labeling for the more deeply buried Cys in peptide **5**. The observation that peptide **3**, which had a Cys deeply buried in the bilayer, was not labeled by any of the ICMT labels shows that the ICMT approach will be able to readily identify Cys in membrane proteins that are deeply buried within lipid bilayers. The lack of labeling for a deeply buried Cys is due to two effects. First, the probes do not penetrate the bilayer. Second, a thiol in a hydrophobic environment will have an elevated p$K_a$ and the level of ionization is expected to be lower than in solution. In aqueous solution, sulfhydryls have a p$K_a$ around 8−9[33,34] and maleimides react with ionized sulfhydryls about 9 orders of magnitude faster than with un-ionized sulfhydryl groups.[35]

We even found that upon disruption of vesicles with mild detergent conditions, the cysteine on peptide **3** still could not be labeled (Figure 5A−D). Labeling was accomplished at 75 °C with the use of sodium cholate to lyse the vesicles. The results suggest that our probes cannot easily permeate detergent micelles in which the cysteine of peptide **3** is buried. The low aggregation number (4−8) of sodium cholate,[19] which should enhance Cys accessibility to external solution in combination with elevated temperature, promoted labeling.

A factor that could complicate interpretation of the labeling data in the case of the specific hydrophobic peptides used in this study is that, although they adopt a transmembrane topology, it was known from fluorescence experiments that a population of peptides that is too small to be detected directly orients parallel to the membrane surface and that sampling of this conformation is rapid, on the second time scale.[18] The orientation of the cysteine with respect to the aqueous probe-containing environment in this conformation depends on whether the $\alpha$-helical structure is strictly maintained and the hydrogen bonding propensity of the midhelix tryptophan, which would be expected to promote a topography in which the Trp faces the aqueous solution. Regardless, the peptides studied are so highly hydrophobic that they should be largely buried within the bilayer when oriented parallel to the membrane surface. Thus, the Cys could remain somewhat


dx.doi.org/10.1021/bc400171j | *Bioconjugate Chem.* 2013, 24, 1235−1247

buried and the probability that it will be labeled could easily be 100- or 1000-fold lower than the probability that the cysteine in transmembrane-oriented peptide **4** would be labeled. Combined with the fact that the nontransmembrane topography only exists for a small fraction of the time that the transmembrane topography is present, labeling of nontransmembrane oriented peptide is expected to make a minor contribution to the labeling in the presence of lipid vesicles. Alternatively, the peptide may simply flip about the center of mass, although this mechanism may be more energetically costly due to burying two sets of charged residues in the membrane simultaneously. Our present experiments cannot distinguish between these two mechanisms.

Nevertheless, the interchange between transmembrane and non-transmembrane topographies did affect the labeling studies in another way. We found that over 90% of peptide **4** could be labeled in intact POPC vesicles within one minute. This strongly suggests that the orientation of the peptide parallel to the lipid bilayer allows flipping of the peptide cysteine orientation. That is, peptides with the cysteine facing the inside of the vesicle rapidly flip so as to reorient the cysteine to the outer bilayer, and vice versa. Through this flipping mechanism, the entire population of peptide **4** cysteine is accessible to probe labeling, regardless of the initial peptide orientation.

This process was readily monitored by adjusting our labeling protocol (Figure 5). We rapidly diluted the first reagent, by addition of an excess of the second probe. Then, the vesicles were lysed in order to label any inaccessible cysteine. Through this modified procedure, we observed the flipping of peptide **4**. Under the conditions of this experiment, the labeling kinetics are determined by both the probe labeling rate and the peptide-flipping rate. This modified procedure is generally useful in cases in which peptides flip rapidly or proteins are peripherally associated with the membrane. It simplifies the labeling experiment because it eliminates the requirements to quench maleimide remaining from the first labeling step and to remove the quench reagent before addition of the second probe.

We also applied our protocol to labeling peptide **4** in different lipid compositions. Addition of 25 mol percent cholesterol to liquid membranes reduced both the peptide labeling and peptide flipping rates. A reduction was also observed upon incorporation of peptide **4** into gel phase membranes. The different membrane phases regulate the flipping rate of transmembrane peptide and our labeling method detects these changes in peptide environment. We attribute the difference in the initial rate of labeling to shifts in relative position of the peptide upon changing the lipid structures. Since cholesterol and the gel phase both increase bilayer width they should decrease Cys accessibility to solvent, which as noted above, slows labeling. Likewise, our labeling protocol detected changes in thiol lipid environment. These changes may also reflect a change in the burial of the thiol group.

## CONCLUSION

We present a method for quantitative analysis of the relative ratios of solvent accessible thiols to membrane buried thiols that requires only microgram quantities of sample and a straightforward experimental protocol. Purification of peptides or lipids after labeling is not required. Reaction mixtures are directly mixed with matrix and analyzed by MALDI-TOF mass spectrometry. There is a minimum of steps involved in the analysis and, consequently, low experimental error. The simplicity of the method makes it amenable to higher throughput sample analysis and faster stopped flow kinetics. The ability of our method to detect the effect of changes in both lipid membrane composition and peptide incorporation on peptide and lipid mobility in the membranes highlights the caution with which the results of biophysical experiments in model systems should be applied to living biological systems with much more complex membranes than typically used in model studies like our own. We expect that our method will be of widespread utility in the future study of membrane-associated proteins in complex cellular contexts due to the simplicity of its application, and the ease with which cysteines can be introduced into native proteins through mutagenesis.

## ASSOCIATED CONTENT

### Supporting Information

Figures and spectra of probes **2a-d$_0$**−**2d-d$_9$** and synthetic intermediates. This material is available free of charge via the Internet at http://pubs.acs.org.

## AUTHOR INFORMATION

### Corresponding Author

*Phone: 631-632-7952. FAX: 631-632-5731. E-mail: nicole.sampson@stonybrook.edu.

### Notes

The authors declare no competing financial interest.

## ACKNOWLEDGMENTS

This work was supported by NSF CHE-1058439 (N.S.S.), NIH R01HL53306 (N.S.S.), NIH S10RR021008 (N.S.S), and NSF MCB-1019986 (E.L.). We thank Hui Tang for initial discussions about this project.

## ABBREVIATIONS

Ac, Acetyl; ALICE, Acid-labile isotope-coded extractants; CHCA, $\alpha$-Cyano-4-hydroxycinnamic acid; CMC, Critical micelle concentration; DPPC, 1,2-Dipalmitoyl-*sn*-glycero-3-phosphocholine; EPR, Electron paramagnetic resonance; EtOAc, Ethyl acetate; ICMT, Isotope-coded mass tag; isotope-ABPP, Isotopic tandem orthogonal proteolysis-activity-based protein profiling; NMR, Nuclear magnetic resonance; PE, Phosphatidylethanolamine; POPC, 1-Palmitoyl-2-oleoyl-*sn*-glycero-3-phosphocholine; PTE, 1,2-Dipalmitoyl-*sn*-glycero-3-phosphothioethanol; SCAM, Substituted-cysteine accessibility methods

## REFERENCES

(1) Hurley, J. H., and Misra, S. (2000) Signaling and subcellular targeting by membrane-binding domains. *Annu. Rev. Biophys. Biomol. Struct. 29*, 49−79.

(2) Malmberg, N. J., and Falke, J. J. (2005) Use of EPR power saturation to analyze the membrane-docking geometries of peripheral proteins: A applications to C2 domains. *Annu. Rev. Biophys. Biomol. Struct. 34*, 71−90.

(3) Altenbach, C., Greenhalgh, D. A., Khorana, H. G., and Hubbell, W. L. (1994) A collision gradient-method to determine the immersion depth of nitroxides in lipid bilayers − application to spin-labeled mutants of bacteriorhodopsin. *Proc. Natl. Acad. Sci. U.S.A. 91*, 1667−1671.

(4) Fanucci, G. E., and Cafiso, D. S. (2006) Recent advances and applications of site-directed spin labeling. *Curr. Opin. Struct. Biol. 16*, 644−653.

(5) Toke, O., Maloy, W. L., Kim, S. J., Blazyk, J., and Schaefer, J. (2004) Secondary structure and lipid contact of a peptide antibiotic in phospholipid bilayers by REDOR. *Biophys. J. 87*, 662−674.
(6) Drechsler, A., and Separovic, F. (2003) Solid-state NMR structure determination. *IUBMB Life 55*, 515−523.
(7) Ladokhin, A. S. (1999) Analysis of protein and peptide penetration into membranes by depth-dependent fluorescence quenching: theoretical considerations. *Biophys. J. 76*, 946−955.
(8) Akabas, M. H., Stauffer, D. A., Xu, M., and Karlin, A. (1992) Acetylcholine-receptor channel structure probed in cysteine-substitution mutants. *Science 258*, 307−310.
(9) Karlin, A., and Akabas, M. H. (1998) Substituted-cysteine accessibility method. *Methods Enzymol. 293*, 123−145.
(10) Woghiren, C., Sharma, B., and Stein, S. (1993) Protected thiol-polyethylene glycol: a new activated polymer for reversible protein modification. *Bioconjugate Chem. 4*, 314−318.
(11) Pomroy, N. C., and Deber, C. M. (1998) Solubilization of hydrophobic peptides by reversible cysteine PEGylation. *Biochem. Biophys. Res. Commun. 245*, 618−621.
(12) Lu, J. L., and Deutsch, C. (2001) Pegylation: A method for assessing topological accessibilities in Kv1.3. *Biochemistry 40*, 13288−13301.
(13) Baessler, K. A., Lee, Y., Roberts, K. S., Facompre, N., and Sampson, N. S. (2006) Multivalent fertilin$\beta$ oligopeptides: the dependence of fertilization inhibition on length and density. *Chem. Biol. 13*, 251−259.
(14) Guy, J., Caron, K., Dufresne, S., Michnick, S. W., Skene, W. G., and Keillor, J. W. (2007) Convergent preparation and photophysical characterization of dimaleimide dansyl fluorogens: elucidation of the maleimide fluorescence quenching mechanism. *J. Am. Chem. Soc. 129*, 11969−11977.
(15) Niwayama, S., Kurono, S., and Matsumoto, H. (2001) Synthesis of d-labeled N-alkylmaleimides and application to quantitative peptide analysis by isotope differential mass spectrometry. *Bioorg. Med. Chem. Lett. 11*, 2257−2261.
(16) van der Veken, P., Dirksen, E. H. C., Ruijter, E., Elgersma, R. C., Heck, A. J. R., Rijkers, D. T. S., Slijper, M., and Liskamp, R. M. J. (2005) Development of a novel chemical probe for the selective enrichment of phosphorylated serine- and threonine-containing peptides. *ChemBioChem 6*, 2271−2280.
(17) Che, F. Y., and Fricker, L. D. (2005) Quantitative peptidomics of mouse pituitary: comparison of different stable isotopic tags. *J. Mass Spectrom. 40*, 238−249.
(18) Ren, J. H., Lew, S., Wang, Z. W., and London, E. (1997) Transmembrane orientation of hydrophobic alpha-helices is regulated both by the relationship of helix length to bilayer thickness and by the cholesterol concentration. *Biochemistry 36*, 10213−10220.
(19) Paula, S., Sus, W., Tuchtenhagen, J., and Blume, A. (1995) Thermodynamics of micelle formation as a function of temperature − a high-sensitivity titration calorimetry study. *J. Phys. Chem. 99*, 11742−11751.
(20) Shahidullah, K., and London, E. (2008) Effect of lipid composition on the topography of membrane-associated hydrophobic helices: Stabilization of transmembrane topography by anionic lipids. *J. Mol. Biol. 379*, 704−718.
(21) Krishnakumar, S. S., and London, E. (2007) The control of transmembrane helix transverse position in membranes by hydrophilic residues. *J. Mol. Biol. 374*, 1251−1269.
(22) McConnell, H. M., and Kornberg, R. D. (1971) Inside-outside transitions of phospholipids in vesicle membranes. *Biochemistry 10*, 1111−1120.
(23) Kol, M. A., de Kroon, A. I. P. M., Rijkers, D. T. S., Killian, J. A., and de Kruijff, B. (2001) Membrane-spanning peptides induce phospholipid flop: a model for phospholipid translocation across the inner membrane of E. coli. *Biochemistry 40*, 10500−10506.
(24) Kol, M. A., van Laak, A. N. C., Rijkers, D. T. S., Killian, J. A., de Kroon, A. I. P. M., and de Kruijff, B. (2003) Phospholipid flop induced by transmembrane peptides in model membranes is modulated by lipid composition. *Biochemistry 42*, 231−237.
(25) Gygi, S. P., Rist, B., Gerber, S. A., Turecek, F., Gelb, M. H., and Aebersold, R. (1999) Quantitative analysis of complex protein mixtures using isotope-coded affinity tags. *Nat. Biotechnol. 17*, 994−999.
(26) Qiu, Y., Sousa, E. A., Hewick, R. M., and Wang, J. H. (2002) Acid-labile isotope-coded extractants: a class of reagents for quantitative mass spectrometric analysis of complex protein mixtures. *Anal. Chem. 74*, 4969−4979.
(27) Weerapana, E., Wang, C., Simon, G. M., Richter, F., Khare, S., Dillon, M. B. D., Bachovchin, D. A., Mowen, K., Baker, D., and Cravatt, B. F. (2010) Quantitative reactivity profiling predicts functional cysteines in proteomes. *Nature 468*, 790−797.
(28) Rogers, L. K., Leinweber, B. L., and Smith, C. V. (2006) Detection of reversible protein thiol modifications in tissues. *Anal. Biochem. 358*, 171−184.
(29) Zhang, R., Sioma, C. S., Wang, S., and Regnier, F. E. (2001) Fractionation of isotopically labeled peptides in quantitative proteomics. *Anal. Chem. 73*, 5142−5149.
(30) Ren, D., Julka, S., Inerowicz, H. D., and Regnier, F. E. (2004) Enrichment of cysteine-containing peptides from tryptic digests using a quaternary amine tag. *Anal. Chem. 76*, 4522−4530.
(31) Li, J., Ma, H. M., Wang, X. C., Xiong, S. X., Dong, S. Y., and Wang, S. J. (2007) Enhanced detection of thiol peptides by matrix-assisted laser desorption/ionization mass spectrometry after selective derivatization with a tailor-made quaternary ammonium tag containing maleimidyl group. *Rapid Commun. Mass Spectrom. 21*, 2608−2612.
(32) Shimada, T., Kuyama, H., Sato, T. A., and Tanaka, K. (2012) Development of iodoacetic acid-based cysteine mass tags: detection enhancement for cysteine-containing peptide by matrix-assisted laser desorption/ionization time-of-flight mass spectrometry. *Anal. Biochem. 421*, 785−787.
(33) Bulaj, G., Kortemme, T., and Goldenberg, D. P. (1998) Ionization-reactivity relationships for cysteine thiols in polypeptides. *Biochemistry 37*, 8965−8972.
(34) Kortemme, T., and Creighton, T. E. (1995) Ionisation of cysteine residues at the termini of model $\alpha$-helical peptides. Relevance to unusual thiol pKa values in proteins of the thioredoxin family. *J. Mol. Biol. 253*, 799−812.
(35) Roberts, D. D., Lewis, S. D., Ballou, D. P., Olson, S. T., and Shafer, J. A. (1986) Reactivity of small thiolate anions and cysteine-25 in papain toward methyl methanethiosulfonate. *Biochemistry 25*, 5595−5601.